DETERMINATION OF NEUTRON SPECTRUM PARAMETERS AT IREN FACILITY USING THE MCNP SIMULATION AND EXPERIMENTAL VALIDATION

by

Le Tran Minh NHAT [1,3]***, Vu Duc CONG*** [2,3]***, Le Hong KHIEM*** [2, 3*]***, Nguyen Thi DINH*** [4]***, Pham Tien THANH*** [2,3]***, Truong Hoai Bao PHI*** [2,5]***, Nguyen Thi Xuan THAI*** [3,4]***, Tran Ngoc TOAN*** [2,5]***, Dinh Van TRUNG*** [2]***, Nguyen Thanh BINH*** [2]***, Nguyen An SON*** [1]***, Valery Nikolaevich SHETSOV*** [3]***, Andrey Yuryevich DMITRIEV*** [3]***, Valerij Vladimirovich LOBACHEV*** [3]***, and Sergey Borisovich BORZAKOV*** [3]

[1] Dalat University, Dalat, Lam Dong, Vietnam
[2] Institute of Physics, Vietnam Academy of Science and Technology, Hanoi, Vietnam
[3] Frank Laboratory of Neutron Physics, Joint Institute of Nuclear Research, Dubna, Rusia
[4] Vietnam Atomic Energy Institute, Hanoi, Vietnam
[5] Dzhelepov Laboratory of Nuclear Problems, Joint Institute of Nuclear Research, Dubna, Russia

Scientific paper
https://doi.org/10.2298/NTRP2501010N

The determination of the characteristics of neutron spectrum at different irradiation positions on the outer wall of moderator chamber of the intense resonance neutron source by simulation method using MCNP code was presented. The characteristics of neutron spectrum including the flux of thermal, epithermal and fast neutron, neutron temperature and α-shape parameter have been determined. For validation of MCNP simulation, the characteristics of neutron spectrum at the optimal irradiation position were determined experimentally by activation technique. The comparison shows that the simulated and experimental results are in agreement, which indicates the high reliability of MCNP code except for α-shape parameter. Our revised equation for determination of α shape parameter by the method of cadmium-ratio for multi-monitor has been used, in which the correction coefficients of the epithermal neutron transmission for cadmium cover, the thermal and epithermal neutron self-shielding, were included for improvement of the accuracy. The calculated and measured α-shape parameters are in good agreement when our proposed revised equation is used.

Key words: intense resonance neutron source, neutron spectrum characterization, MCNP, activation method

INTRODUCTION

Neutron-induced nuclear reaction cross-section data, particularly in the thermal and resonance regions, serve as a fundamental basis for both basic research and practical applications. In nuclear safety, accurate cross-section data are essential for optimal reactor design, enabling reliable performance predictions and chain reaction control. Similarly, medical applications including radioisotope production for diagnostic imaging or cancer treatment, depend critically on neutron cross-section reliability at specific energies. Although numerous evaluated nuclear data libraries exist, the demand for improved accuracy persists [1], especially for isotopes exhibiting complex resonance structures in the epithermal range (1 eV-100 keV).

* Corresponding author, e-mail: lhkhiem@iop.vast.vn

At the Joint Institute for Nuclear Research (JINR), the intense resonance neutron source IREN based on the LUE-200 electron linear accelerator [2-4] has emerged as a powerful tool for high-resolution neutron studies. Unlike conventional reactor sources relying on moderated fission neutrons, IREN generates neutrons predominantly through the photoneutron mechanism when 110 MeV electron beams interact with a tungsten target. While this design offers advantages for resonance studies, it simultaneously introduces challenges in characterizing the neutron flux distribution at irradiation positions. Key spectral parameters such as the relative contributions of thermal, epithermal, and fast neutrons, the epithermal spectrum shape parameter α, and the neutron temperature, must be known in advance to ensure precise cross-section measurements.

Numerous previous studies have focused on determining neutron spectral parameters using various

methodological approaches, depending on the type of neutron source and the specific research context. For example, Khattab *et al*. [5] and Akaho *et al*. [6] employed MCNP simulations to calculate neutron spectra in MNSR reactors. This approach was also adopted by Beasley *et al*. [7] to characterize the epithermal neutron spectrum of the Portuguese research reactor. Dias *et al*. [8] applied covariance analysis to determine the α-shape parameter in k_o-based neutron activation analysis (k_o-NAA). Yavar *et al*. [9] and Soleimani *et al*. [10] compared MCNP simulation results with experimental data to calibrate spectral parameters in research reactors. Additionally, Alloni *et al*. [11] characterized neutron fields generated by accelerators through a combination of simulations and experimental measurements. In the context of accelerator-driven neutron sources, Alloni *et al*. [11] demonstrated that significant errors in intermediate-energy neutron modeling may arise if multiple scattering in target materials is neglected. Devan *et al.* [12] conducted a study to investigate the photoneutrons produced by the Pohang Neutron Facility, based on an electron linac in the watercooled Ta-target system using the Monte Carlo simulation code MCNPX. The maximum energy of the electron linac is 75 MeV. Multiple gold foil neutron activation experiments were carried out to estimate the spatial distribution of photo-neutrons. The optimum conditions of the target system and the experimental set-up to maximize the thermal neutron production, were investigated. Notably, in a comprehensive review on photoneutron production from electron accelerators, Sari [13] highlighted that uncertainties in nuclear cross-section libraries can lead to substantial discrepancies in predicted fast neutron fluxes.

Our research group is the first to propose the use of the IREN facility for measuring neutron-induced nuclear reaction cross sections via the activation method. To ensure the accuracy of the results, the initial and essential task is to precisely characterize the neutron flux at the sample irradiation positions. The objective of this study is to determine key characteristics of the neutron flux at sample irradiation positions using the Monte Carlo method implemented in the MCNP code [14]. The accuracy of the simulation results is evaluated by comparison with corresponding experimental data obtained through the activation method. Additionally, the study aims to identify and apply necessary corrections to improve the accuracy of neutron flux parameters determined experimentally.

MATERIAL AND METHODS

Neutron production by IREN

The principle of neutron production of IREN facility is based on (e, γ) and (γ, n), (γ, xn) and (γ, xnyp) nuclear reactions. The electrons accelerated to high energy from a linear accelerator are used to bombard a photoneutron target to create bremsstrahlung radiation, which then generates neutrons via photonuclear reactions with the target material. The photoneutron target should be made from heavy metal with high atomic number because the emission of gamma rays is proportional to the atomic number of the target material. The IREN facility consists of the electron linac LUE200 with an S-band traveling wave accelerating structure [15]. The electrons exit the accelerator through a window made of hemispherical beryllium with a diameter of 36 mm and a thickness of 1 mm.

The general schematic of the IREN facility is presented in fig. 1.

The currently achieved parameters of an electron beam accelerated by the LUE-200 accelerator are given in tab. 1.

For converting bremsstrahlung into neutron radiation, a cylindrical tungsten alloy (90 % W, 7 % Ni, 3 % Fe, ρ = 18.075 gcm^{-3}) of 4 cm diameter and 10 cm length has been used as a neutron production target. The tungsten target is placed inside an aluminum cy-

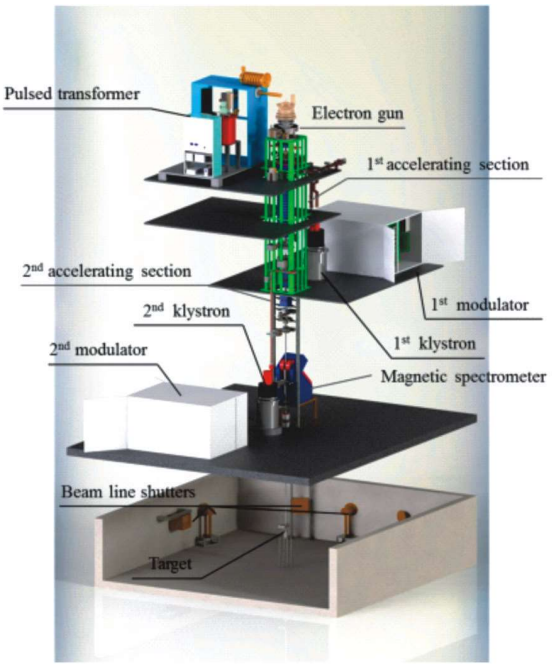

Figure 1. The general schematic of IREN

Table 1. The currently achieved parameters of the electron beam accelerated by the LUE-200 accelerator used for simulation

Average electron energy	110 ± 5 MeV
Pulse beam current	1.8 A
Average current	10.8 μA
Pulse duration	120 ns
Cycle repetition rate	50 Hz
Average power on target	1.2 kW

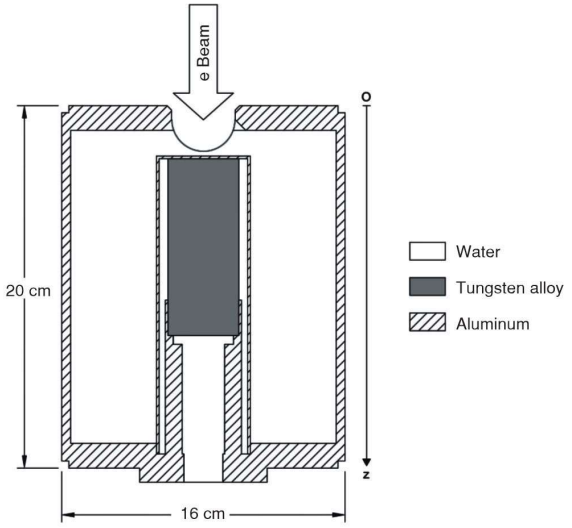

Figure 2. The design of neutron irradiation chamber

lindrical container of 16 cm diameter and 25 cm length, containing distilled water to moderate the produced neutrons. The production target is continuously cooled by circulating water in the moderator tank using a pump. In fig. 2, the design of neutron irradiation chamber, including tungsten target and water moderator tank, is presented.

Monte Carlo simulation of neutron spectra using MCNP code

For measurement of the cross-section of the reactions induced by thermal and epithermal neutrons, the reaction targets made by high-purity metal thin foils will be used and will be attached to some position on the outer wall of the water moderator tank, as presented in fig. 3(a). Before the experiment, one should know the main characteristic quantities of neutron spectrum at a selected irradiation position as accurate as possible. These quantities can be deduced from the neutron spectrum at the corresponding position and therefore, it is necessary to know accurate neutron energy spectra, either by experimental measurement or by simulation.

In our study, the neutron energy spectra have been simulated by the Monte Carlo method using MCNP-6 code. Figure 3(a) shows a horizontal cross-section of the configuration of irradiation chamber used for MCNP simulation, where the vertical direction of Z-axis is sketched, which is directed downwards from the top of the water moderator tank coinciding with the direction of the incoming electron beame. The point with $z = 0$ is the one located on the top surface of the water moderator tank. The currently achieved parameters of the electron beam accelerated by the LUE-200 accelerator are presented in tab. 2 and the energy distribution of electron beam, measured in October 2023 which is presented in fig. 3(b), have been used for simulation. For each simulation, 10^9 events have been generated.

Gamma activity measurement and determination of reaction rate

To measure the activity of neutron-activated targets, a high-energy-resolution gamma spectrometer was used. The detector used to record the gamma-ray spectrum is the HPGe detector of GC4018 model manufactured by Canberra, with 40 % relative efficiency

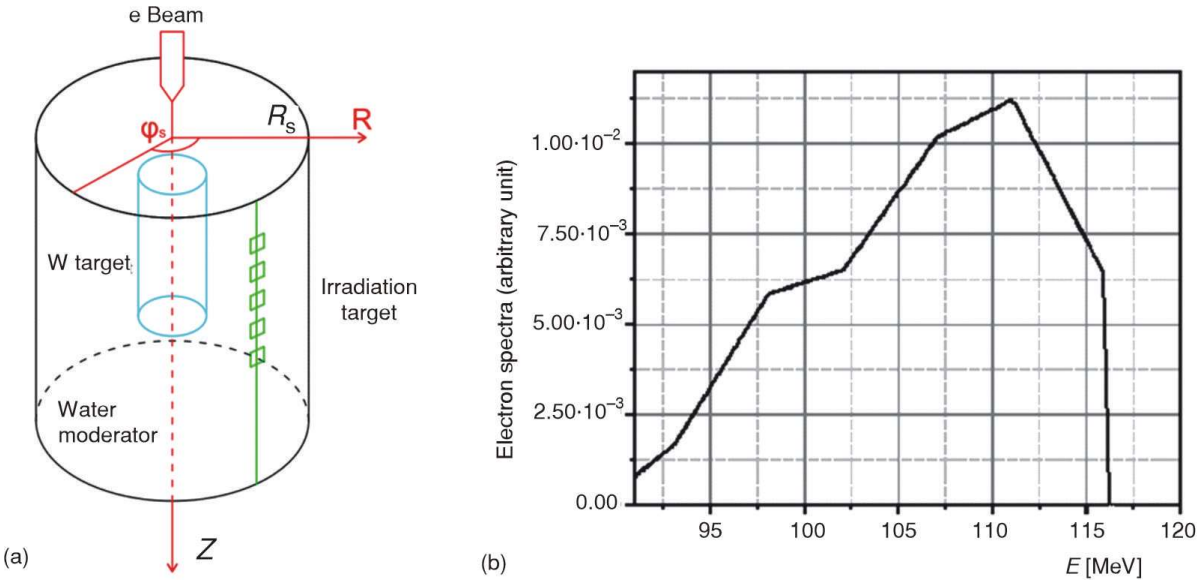

Figure 3. The configuration of neutron production chamber (a) and the energy distribution of electron beam measured in October 2023 (b) for MCNP simulation

Table 2. The neutron self-shielding coefficients of some isotopes present in the targets will be used in our experiment for comparison

Target	Size [mm]	Thickness [mm]	Nuclide	G_{th}	G_{epi}	G_{fast}
Au	9 × 9	0.1	^{197}Au	0.8837	0.2142	0.2142
Cu	13 × 11	0.5	^{63}Cu	0.9659	0.6980	0.6975
Zr	10 × 9	0.1	^{94}Zr	0.9997	0.9812	0.9811
Zr	10 × 9	0.1	^{96}Zr	0.9997	0.9773	0.9767
W	10 × 9	0.35	^{186}W	0.9168	0.2524	0.2379
W	10 × 9	0.35	^{184}W	0.9168	0.6112	0.5973

and energy resolution of 1.8 keV at 1.33 MeV. The reaction rate per target nucleus is determined by the following formula [16]

$$R = F_c \frac{N_{obs}\lambda(1-e^{-\lambda t_{cp}})}{n_0 \varepsilon I_\gamma (1-e^{-\lambda\tau})(1-e^{-\lambda\tau_t})\, e^{-\lambda\tau_w}(1-e^{-\lambda\tau_c})} \quad (1)$$

where R is reaction rate per target nucleus, n_0 – the number of nuclei of the target, ε – the detector's efficiency at the energy of the characteristic gamma peak, N_{obs} – the gamma-ray count at the characteristic energy peak, I_γ – the gamma emission intensity, λ – the decay constant, t_{cp} – the cycle period of the electron beam, τ – the pulse width of the electron beam, t_i – the time of irradiation, t_w – the cooling time, t_c – the time of measurement, and F_c – the general correction factor for gamma measurement, including efficiency geometrical correction, gamma self-absorption in the target, dead time correction and summing effect. For correction of losses of gamma-ray count of interest, gamma-ray characteristic energy peak due to an effect of true coincidence summing, a correction program TrueCoinc [17] has been used. For determination of gamma self-absorption in the target and for efficient geometrical correction, two different Monte Carlo codes, developed by us, have been used.

In this study, high purity natural Am and Cu samples (> 99.9 %) were used. The activities of the isotopes ^{198}Au and ^{64}Cu produced via the ^{197}Au(n,γ)^{198}Au and ^{63}Cu(n,γ)^{64}Cu reactions were determined using the gamma peaks of 411.80 keV (95.62 %) for ^{198}Au and the 1345.37 keV (0.4748 %) for ^{64}Cu. The sample measurement time was adjusted to achieve a statistical uncertainty of less than 1 %.

RESULTS AND DISCUSSIONS

All the necessary quantities characterizing the neutron spectra at an irradiation position will be deduced from the neutron spectra at this site. The neutron spectra at different irradiation positions located on the outer wall of the water moderator tank, with and without cadmium cover, have been simulated. Three typical different neutron energy spectra are presented in fig. 4, corresponding to three cases: without cadmium cover (represented by a solid circle), with cadmium cover of 0.5 mm thickness (solid triangle), and 1 mm thickness (solid square). One can see clearly from fig. 4 that the spectra of the targets with cadmium cover of 0.5 mm and 1 mm thickness are almost identical. This means that the absorption of thermal neutrons by cadmium cover with these two thicknesses of 0.5 mm and 1 mm is equivalent. Therefore, it can be concluded that to completely absorb completely thermal neutrons, a cadmium cover with thickness of 0.5 mm is sufficient.

Selection of optimal position for irradiation

The optimal irradiation positions must be selected to increase the activity of irradiated targets. The optimal irradiation positions are those at which the induced reaction rates should be the highest. To find the

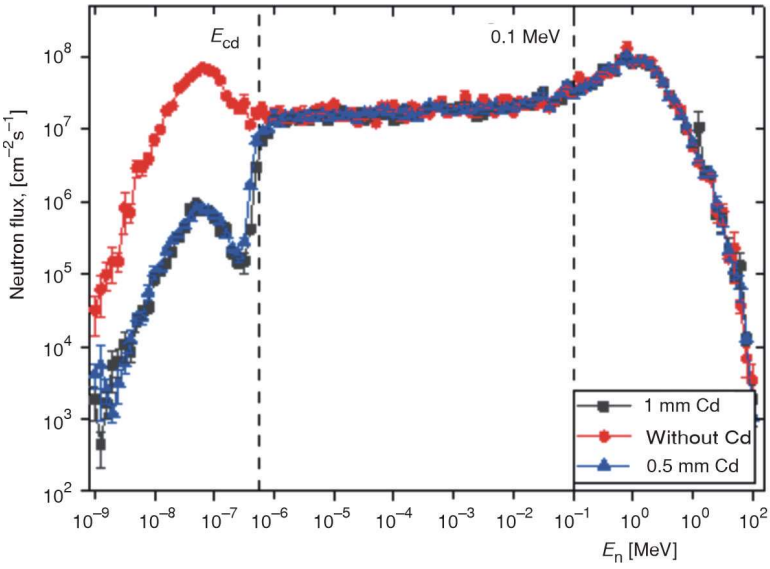

Figure 4. The neutron spectra simulated by MCNP at an irradiation site Z = 5 cm

optimal irradiation positions, the reaction rates of some isotopes at different irradiation vertical positions Z should be calculated. The reaction rates induced by thermal, epithermal and fast neutrons can be calculated using the following formulas [18]

$$R_{\text{th}} = G_{\text{th}} \int_{0}^{E_{\text{Cd}}} \varphi(E_{\text{n}})\sigma(E_{\text{n}})\text{d}E_{\text{n}} \quad (2)$$

$$R_{\text{epi}} = G_{\text{epi}} \int_{E_{\text{Cd}}}^{E_{\text{f}}} \varphi(E_{\text{n}})\sigma(E_{\text{n}})\text{d}E_{\text{n}} \quad (3)$$

$$R_{\text{fast}} = G_{\text{fast}} \int_{E_{f}}^{\infty} \varphi(E_{\text{n}})\sigma(E_{\text{n}})\text{d}E_{\text{n}} \quad (4)$$

where $\varphi(E_{\text{n}})$ is the neutron flux and $\sigma(E_{\text{n}})$ – the reaction cross-section at neutron energy of E_{n}, R_{th}, R_{epi}. The and R_{fast} are the reaction rates induced by thermal, epithermal. The and fast neutrons at a specific irradiation position, G_{th}, G_{epi}, and G_{fast} are the thermal, epithermal, and fast self-shielding correction factors and $E_{\text{cd}} = 0.55$ eV is the cadmium cutoff energy and $E_{\text{f}} = 0.1$ MeV.

The total reaction rate R_{tot} will be the sum of these three reaction rates and is calculated using the following formula

$$R_{\text{tot}} = R_{\text{th}} + R_{\text{epi}} + R_{\text{fast}} \quad (5)$$

Table 2 shows the calculated values of the coefficients of G_{th}, G_{epi}, and G_{fast} for nuclides ^{197}Au and ^{63}Cu, that are present in our pure natural metal foils used in experimental measurement for validation of MCNP simulated results. These coefficients were calculated based on the method described by Trkov [19] and the values of $\sigma(E_{\text{n}})$ were taken from the ENDF/B-VIII.0 library.

Figure 5 presents the relationship of the reaction rate calculated for ^{63}Cu to the irradiation positions at different Z. It should be noted that for calculation of reaction rates using eqs. (2-5), the neutron flux at diferent irradiation positions calculated by MCNP were used. It can be seen clearly from fig. 5 that the optimal irradiation position in the Z direction will be the point with $Z = 5$ cm.

Determination of characteristic parameters of the neutron spectrum at the optimal irradiation position $Z = 5$ cm

A neutron energy spectrum at an irradiation site can be divided into three regions including:

The thermal region with neutron energy less than cadmium cut-off energy $E_{\text{Cd}} \approx 0.55$ eV, which can be described by the following function [20]

$$\varphi_{\text{th}}(E_{\text{n}}) = \Phi_1 \frac{E_{\text{n}}}{(kT_{\text{th}})^2} \text{e}^{-E_{\text{n}}/kT_{\text{th}}} \quad (6)$$

where E_{n} is the neutron energy, k – the Boltzmann constant, and T_{th} is average neutron temperature (or Maxwellian temperature).

The epithermal region with neutron energy $E_{\text{Cd}} \le E \le E_{\text{f}} = 0.1$ MeV, which can be described by the following function [20, 21]

$$\varphi_{\text{epi}}(E_{\text{n}}) = \frac{\Phi_2}{E_{\text{n}}^{1+a}} \quad (7)$$

where α is the epithermal spectrum shape parameter.

The fast region in which neutron energy is greater than E_{f} can be approximated by the Maxwellian distribution, as written [20]

$$\varphi_{\text{fast}}(E_n) = \Phi_3 \frac{E_n}{(kT_{\text{f}})^2} \text{e}^{-E_{\text{n}}/kT_{\text{f}}} \quad (8)$$

where T_{f} is the average temperature of fast neutrons, Φ_1, Φ_2, and Φ_3 in the eqs. (6)-(8) are the flux of thermal, epithermal, and fast neutrons and their unit is in $\text{cm}^{-2}\text{s}^{-1}$. The total energy neutron spectrum will be the sum of three individual energy spectra (6-8) aforementioned.

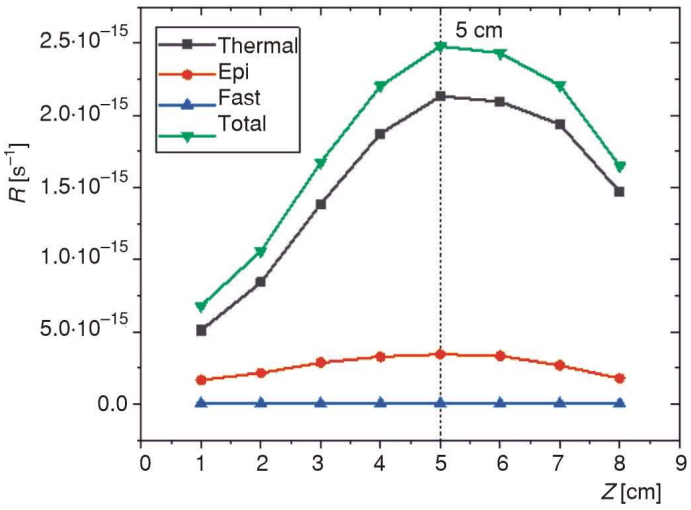

Figure 5. The relationship of the reaction rate calculated for ^{63}Cu to the irradiation position Z

The characteristic parameters of the neutron spectrum, at a specific irradiation position, include $\Phi_1, \Phi_2, \Phi_3, T_{th}, \alpha$, and T_f. These parameters can be obtained if the measured or simulated spectra at the corresponding irradiation position are available. In our case, neutron energy spectra have been simulated using MCNP code. To deduce the characteristic parameters, one needs to fit the distributions (6-8) correspondingly with the thermal ($E_n \leq 0.55$ eV), epithermal (0.55 eV < $E_n \leq 0.1$ MeV), and fast ($E_n \geq 0.1$ MeV) energy regions, namely: the values of Φ_1 and T_{th} can be obtained by fitting the distribution (6) to the simulated spectrum in the region with neutron energy less than E_{cd} (0.55 eV), the values of Φ_2 and α can be obtained by fitting the distribution (7) to the simulated spectrum in the region with neutron energy $E_{cd} \leq E_n \leq 0.1$ MeV and the values of Φ_3 and T_f can be obtained by fitting the distribution (8) to the simulated spectrum in the region with neutron energy $E_n > 0.1$ MeV. The MCNP simulated neutron flux density spectrum at the irradiation position $Z = 5$ cm and the fitting curves, are presented in fig. 6. In this figure, the values simulated by MCNP are represented by the solid squares, the dashed line is the fitting curve of distribution (6) to the MCNP simulated points for determination of Φ_1 and kT_{th}, the solid line is the fitting curve of distribution (7) to the MCNP simulated points for determination of Φ_2 and α shape parameter, and the dotted line is the fitting curve of distribution (8) to the MCNP simulated points for determination of Φ_3 and kT_f. The obtained results are listed in tab. 3.

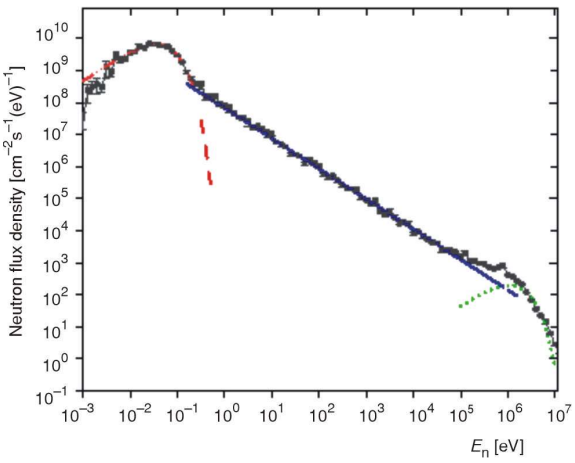

Figure 6. Fitting curves in three energy regions of neutron flux density spectrum at the irradiation position $Z = 5$ cm

It can be seen from tab. 3 that the values of α-shape parameter and Maxwellian neutron temperature T_n are very different at different sample irradiation positions. Their magnitudes of the discrepancies at different irradiation positions can be observed more clearly in fig. 7. The value of α-shape parameter increases with the value

Table 3. The characteristic parameters of the neutron spectrum at different irradiation positions for the case without cadmium cover

Z [cm]	Φ_1 [10^8 cm^{-2}s^{-1}]	Φ_2 [10^8 cm^{-2}s^{-1}]	Φ_3 [10^8 cm^{-2}s^{-1}]	kT_{th} [meV]	α	kT_f [MeV]
1	1.627	1.038	5.236	41.064	–0.1062	1.133
2	2.590	1.158	5.939	38.863	–0.0898	1.067
3	4.261	1.361	7.763	38.761	–0.0722	0.868
4	5.833	1.402	7.266	39.078	–0.0580	1.041
5	6.451	1.420	4.767	36.611	–0.0550	1.244
6	6.480	1.458	6.942	37.887	–0.0588	0.874
7	5.917	1.008	5.331	36.902	–0.0419	1.043
8	4.166	0.729	3.494	32.673	–0.0551	1.178

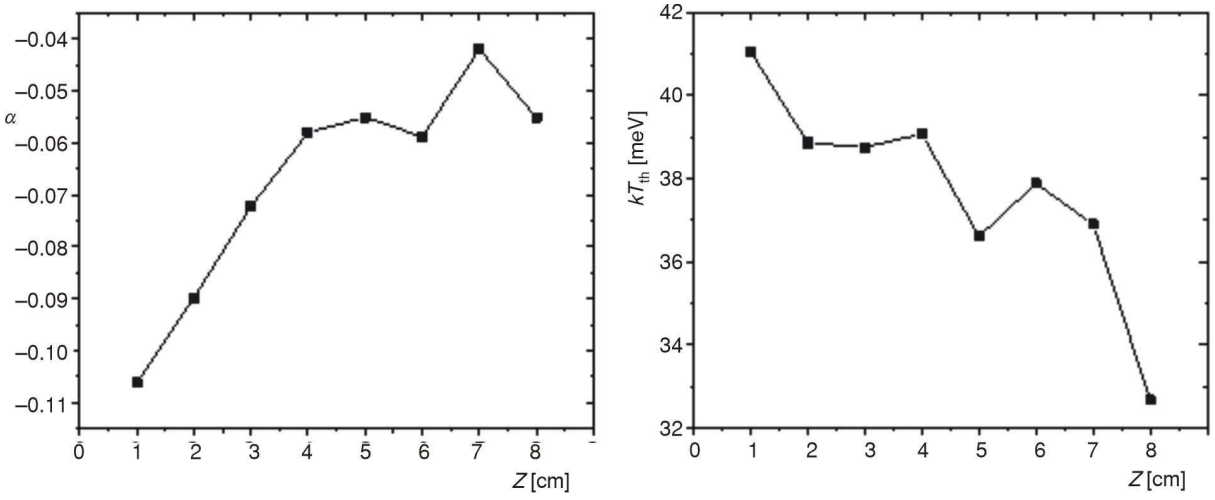

Figure 7. The variation of a shape parameter and T_n at different irradiation positions

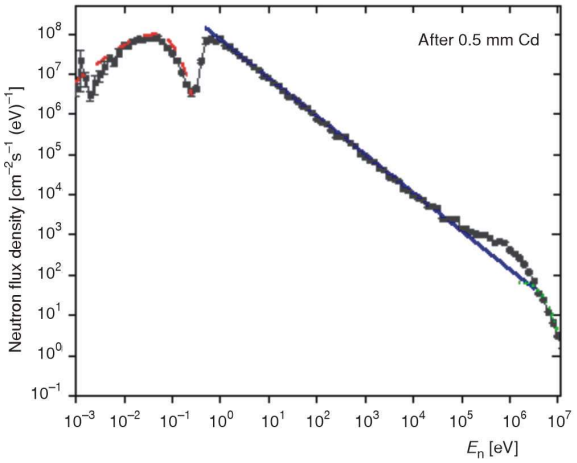

Figure 8. The simulated neutron density spectrum after 0.5 mm cadmium cover at the irradiation position $Z = 5$ cm and the fitting curves

of Z, while the temperature T_{th} decreases with increasing Z. This is quite consistent with our prediction because the larger the distance Z corresponds to the layer thickness of the water layer. The greater the thickness of the neutron-slowing water layer, the better the neutron thermalization process and thus will reduce the deviation of the neutron spectrum from the ideal 1/E spectrum and reduce the neutron temperature T_{th}.

The MCNP simulated neutron spectrum after 0.5 mm cadmium cover at the irradiation position $Z = 5$ cm and the fitting curves are presented in fig. 8. In this figure, the points simulated by MCNP are represented by the solid squares, the dashed line is the fitting curve of distribution (6) to the MCNP simulated points for determination of Φ_1^{cd} and kT_{th}^{cd}, the solid line is the fitting curve of distribution (7) to the MCNP simulated points for determination of Φ_2^{cd} and kT_{th}^{cd}, and the dotted line is the fitting curve of distribution (8) to the MCNP simulated points for determination of Φ_3^{cd} and kT_{th}^{cd}.

The characteristic parameters of the neutron spectrum at the irradiation position $Z = 5$ cm after cadmium cover of 0.5 mm thickness, are listed in tab. 4 in which the superscript cd of each quantity is used for cadmium covered target, for example, Φ_2^{cd}, Φ_2^{cd} and Φ_2^{cd} and the thermal, epithermal and fast neutron fluxes after the cadmium cover.

Determination of cadmium rati by MCNP simulation

The cadmium ratio (CR) is defined as the ratio of reaction rates of the targets without and with the cadmium cover as follows [22, 23]

$$CR = \frac{R^{bare}}{R^{cd}} = \frac{\int_0^{\infty} \sigma_\gamma(E)\varphi(E)\mathrm{d}E}{\int_{E_{cd}}^{\infty} \sigma_\gamma(E)\varphi(E)\mathrm{d}E} \quad (9)$$

where R^{bare} and R^{cd} are the reaction rates of bare and cadmium covered targets, $\sigma_\gamma(E)$ and $\varphi(E)$ are the neutron capture cross section and neutron flux at energy E, respectively, and E_{cd} – the cadmium cutoff energy. This formula is correct under the assumption that all neutrons with energies less than E_{cd} will be completely absorbed by the cadmium cover. It is known that the CR can be calculated if the neutron energy spectrum can be measured experimentally or can be calculated for the target with and without cadmium cover.

For calculation of CR, the MCNP simulated spectrum presented in fig. 5 and the neutron self-shielding thermal and epithermal coefficients taken from tab. 2 were used. The calculated results of CR for some targets assuming that $E_{cd} = 0.55$ eV and the thickness of used cadmium cover of 0.5 mm are listed in tab. 5, in which R^{bare} and R^{cd} are the reaction rates of the targets induced by thermal, epithermal and fast neutrons without and with 0.5 mm cadmium cover.

Verification of accuracy of the characteristic parameters calculated from MCNP simulated neutron spectra

To verify the accuracy of the characteristic parameters calculated from MCNP simulated neutron spectra, three experiments were carried out. The first experiment aims to check the optimal irradiation position, where the neutron flux is the highest. In this experiment, the 10 mm × 10 mm × 0.5 mm thin Cu targets of high purity (> 99.99 %) were activated at five irradiation positions, located on the outside wall of the moderator tank with $Z = 1, 3, 5, 7, 9$ cm. The gamma-ray spectra of the irradiated targets were measured using our gamma-ray spectrometer, mentioned above. The measured reaction rates per target nucleus of ^{63}Cu isotope of the Cu targets, with and without cadmium cover, at different irradiation positions, directly determined from measured gamma-ray spectra using eq. (1) are listed in tab. 6, where R^{cd} and R^{bare} are the reaction rates of the target with and without cadmium cover, respectively.

In fig. 9, the relationship between reaction rate and irradiation position at different Z is presented.

Table 4. The characteristic parameters of the neutron spectrum at the irradiation position $z = 5$ cm for the case with the cadmium cover of 0.5 mm thickness

Z [cm]	Φ_1^{cd} (10^8 cm^{-2} s^{-1})	Φ_2^{cd} (10^8 cm^{-2} s^{-1})	Φ_3^{cd} (10^8 cm^{-2} s^{-1})	kT_{th}^{cd} [meV]	α	kT_{th}^{cd} [meV]
5	0.106	1.614	7.797	39.310	–0.058	0.194

Table 5. The calculated results of CR for some targets assuming the cadmium cut-off energy is 0.55 eV and the thickness of used cadmium cover is 0.5 mm

Nuclide	Reaction rate of bare target (R^{bare}) [s^{-1}]	Reaction rate of cadmium covered target (R^{cd}) [s^{-1}]	CR
^{197}Au	$6.66\cdot10^{-14}$	$2.49\cdot10^{-14}$	2.675
^{94}Zr	$7.45\cdot10^{-17}$	$5.49\cdot10^{-17}$	1.357
^{96}Zr	$5.28\cdot10^{-16}$	$5.58\cdot10^{-16}$	0.946
^{63}Cu	$2.48\cdot10^{-15}$	$4.08\cdot10^{-15}$	6.086
^{186}W	$2.66\cdot10^{-14}$	$1.02\cdot10^{-14}$	2.600
^{184}W	$1.79\cdot10^{-15}$	$1.14\cdot10^{-15}$	1.564

Table 6. The measured reaction rate per target nucleus of ^{63}Cu isotope at different irradiation positions

Z [cm]	R^{bare} [s^{-1}]	R^{cd} [s^{-1}]
1	$3.78\cdot10^{-16}\pm2.49\cdot10^{-18}$	$8.45\cdot10^{-17}\pm7.28\cdot10^{-19}$
3	$7.72\cdot10^{-16}\pm4.93\cdot10^{-18}$	$1.19\cdot10^{-16}\pm1.02\cdot10^{-18}$
5	$1.03\cdot10^{-15}\pm6.58\cdot10^{-18}$	$1.34\cdot10^{-16}\pm1.23\cdot10^{-18}$
7	$9.44\cdot10^{-16}\pm6.19\cdot10^{-18}$	$1.39\cdot10^{-16}\pm1.31\cdot10^{-18}$
9	$7.16\cdot10^{-16}\pm4.88\cdot10^{-18}$	$1.09\cdot10^{-16}\pm1.20\cdot10^{-18}$

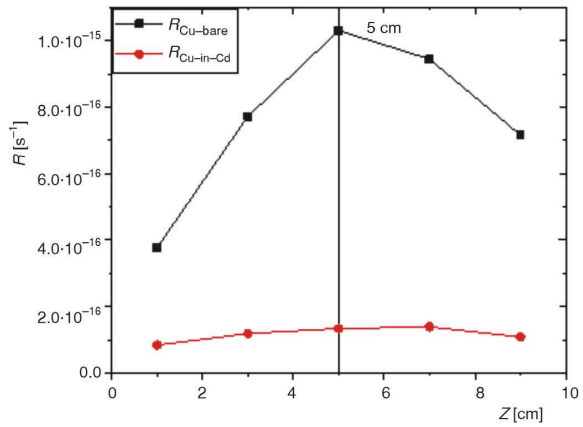

Figure 9. Relationship between reaction rate per nucleus of ^{63}Cu and irradiation position at different z

The results listed in tab. 6 and shown in fig. 9 indicate that the irradiation position at Z = 5cm gives the highest reaction rate. This experimental conclusion is completely consistent with the results obtained by the simulation presented above. In addition, the agreement between the simulation and experimental results allows us to conclude that the MCNP code can accurately simulate the neutron spectra at different irradiation positions.

The second experiment aims to compare the cadmium ratio obtained by simulation and by measurement. In this experiment, the high purity (>99.9 %) thin natural metal foils of gold and copper were used as the targets for neutron irradiation. The two sets of targets, without and with 0.5 mm thickness cadmium cover, were prepared for simultaneous irradiation at the optimal irradiation positions Z = 5 cm located on the outer wall of the moderator. The targets were simultaneously activated by neutron at the optimal irradiation position with Z = 5 cm. The gamma spectra emitted by the targets after irradiation were recorded using the gamma spectrometer described in section 2.3 and analyzed using Genie-2000 software. The counting rates at characteristic peaks (at 411.8 keV for ^{198}Au and 1345.37 keV for ^{64}Cu), after taking into account all the necessary corrections, were used to calculate the CR of ^{197}Au and ^{63}Cu isotopes. The reaction rates per target nucleus of the isotopes ^{197}Au and ^{63}Cu were determined experimentally by the activation method. The CR were determined from the measured reaction rates and are given in tab. 7, where CR_{exp} and CR_{cal} are the experimental and calculated CR, respectively. The values of CR_{cal} are taken from tab. 5.

Table 7. The CR determined experimentally for diferent targets and compared with the values obtained by simulation

Nuclide	CR_{exp}	CR_{cal}	Difference [%]
^{197}Au	2.58 ±0.06	2.675	3.72
^{63}Cu	6.33 ±0.08	6.086	3.91

The calculated CR listed in tab. 5, that were deduced from MCNP simulated spectra are also given in this table for comparison. The results in tab. 7 show that the CR calculated by simulation and measured by experiment are relatively consistent. This once again allows us to conclude that the method of determining the CR using MCNP simulation is relatively accurate and acceptable instead of time-consuming experimental measurements.

The third experiment is for comparison of experimental α-shape parameter with that deduced from MCNP simulated neutron spectrum.

The value of α-shape parameter can be experimentally determined by the CR for multimonitor method [21, 24]. For determination the value of α shape parameter, the CR method has been used using the obtained experimental values of CR_{exp} listed in tab. 7.

The determination of the α-shape parameter is based on the ratio of epithermal neutron-induced reaction rates measured in two different monitor foils. To eliminate dependence on absolute nuclear data, De Corte *et al.* [21] reformulated the α-determination equation by dual monitor method using CR However, their initial formulation did not account for several corrections, such as the correction of cadmium transmission and correction of the thermal and epithermal

neutron selfshielding. Subsequent studies [25, 26] incorporated these corrections, leading to a more comprehensive expression of the form

$$\frac{(\mathrm{CR}^{*}-1)_{\mathrm{Au}}}{(\mathrm{CR}^{*}-1)_{\mathrm{W}}}=\frac{[(Q_0-0.4264)G]_{\mathrm{W}}(\overline{E}_{\mathrm{r,W}})^{-\alpha}+C_{\alpha}}{[(Q_0-0.4264)G]_{\mathrm{Au}}(\overline{E}_{\mathrm{r,Au}})^{-\alpha}+C_{\alpha}} \tag{10}$$

where

$$\mathrm{CR}^{*}=\mathrm{CR}/F_{\mathrm{cd}},C_{\alpha}=0.4264/(2\alpha+1)E_{\mathrm{cd}}^{\alpha},$$
$$Q_0=I_0/g\sigma_0,G=G_{\mathrm{epi}}/G_{\mathrm{th}}$$

where CR is cadmium ratio, F_{cd} – the cadmium transmittance coefficient, $E_{\mathrm{cd}}=0.55$ eV – the effective cadmium cut-off energy, G_{th} and G_{epi} are corrections for thermal and epithermal self-shielding effects, σ_0 – the cross- section of the thermal neutron capture reaction at a speed of 2200 ms^{-1}, I_0 – the integral cross-section of the resonance neutron capture reaction, and $\overline{E}_r$ – the average energy of all the neutron resonances. The subscripts Au and W refer to gold and tungsten monitors, respectively.

By very careful transformations, we have proposed another equation for determination of α-shape parameter by the dual monitor method using CR in which the correction factors F_{cd}, G_{th}, and G_{epi}, were included

$$\frac{(\mathrm{CR}^{*}-1)_2}{(\mathrm{CR}^{*}-1)_1}\cdot\frac{G_2}{G_1}=\frac{[(Q_0-0.426)(\overline{E}_r)^{-\alpha}]_1+C_{\alpha}}{[(Q_0-0.426)(\overline{E}_r)^{-\alpha}]_2+C_{\alpha}} \tag{11}$$

where

$$\mathrm{CR}^{*}=\mathrm{CR}/F_{\mathrm{cd}},Q_a=I_0/g\sigma_0,$$
$$C_{\alpha}=0.4264/(2\alpha+1)E_{Cd}^{\alpha},G=G_{\mathrm{epi}}/G_{\mathrm{th}}$$

To calculate G_{epi} and G_{th}, several studies have proposed methods for estimating these quantities [27, 28]. Trkov *et al*. [19] developed the MATSSF code using an analytical approach to approximate the solution of the neutron diffusion equation for neutron self-shielding correction calculations, including the thermal (G_{th}) and epithermal (G_{epi}) self-shielding factors. A detailed description of the methodology and the relevant computational equations is provided in [19]. The MATSSF code offers the advantage of fast computation and is capable of handling samples composed of various elemental constituents. It supports several predefined sample geometries, including thin foil, cylindrical, and spherical shapes. The authors employed both the MATSSF code and the MCNP code to perform calculations, and the results obtained from both methods were found to be in very good agreement. Therefore, in this study, we used the MATSSF code to determine the neutron selfshielding factors for the Au and Cu samples used in the present study.

The α-shape parameter can be obtained by solving eq. (11) by the iterative method using the experimental CR taken from tab. 7 and the relevant nuclear data listed in tab. 8. We also used the equations proposed in [25, 26, 29] to determine the α-shape parameter. The values of the α-shape parameter obtained from different equations are presented in tab. 9.

Through this study, we observed that the values of the α-shape parameter vary depending on the monitor pair used. In our opinion, in addition to the systematic errors of the input data taken from tab. 8, there may also be some other causes related to the neutron spectrum such as, the cadmium cover does not completely absorb thermal neutrons and the contribution of fast neutrons in the epithermal region is quite large.

The value of the α shape parameter determined by eq. (11) depends on many parameters. The errors of these quantities will be propagated to the final α value. In addition, we found that the value of α -shape parameter is very sensitive to some parameters such as F_{cd} (cadmium transmission coefficient), CR, G_{th} and G_{epi} (thermal and epithermal neutron self-shielding coefficients), and Q_0. Even a very small change in these parameters can lead to a large change in the value of the α-shape parameter.

To reduce errors caused by the previous two phenomena, we have proposed two new correction factors in the calculation. The first correction factor $C_{\mathrm{f}}^{\mathrm{bare}}$ is for correcting the influence of fast neutrons on the reaction rate of the bare target. The second correction factor $C_{\mathrm{tf}}^{\mathrm{cd}}$ takes into account the influence of residual thermal neutrons passing through the cadmium cover and of fast neutrons, on the reaction rate of the cadmium covered target. The coefficients $C_{\mathrm{f}}^{\mathrm{bare}}$ and $C_{\mathrm{tf}}^{\mathrm{cd}}$ are defined as follows

$$C_{\mathrm{f}}^{\mathrm{bare}}=\frac{R_{\mathrm{fast}}^{\mathrm{bare}}}{R_{\mathrm{tot}}^{\mathrm{bare}}} \tag{12}$$

$$C_{\mathrm{tf}}^{\mathrm{cd}}=\frac{R_{\mathrm{th}}^{\mathrm{cd}}+R_{\mathrm{fast}}^{\mathrm{cd}}}{R_{\mathrm{tot}}^{\mathrm{cd}}} \tag{13}$$

where $R_{\mathrm{fast}}^{\mathrm{bare}}$ and $R_{\mathrm{tot}}^{\mathrm{bare}}$ are the reaction rates induced by fast neutrons and all neutrons (thermal, epithermal and fast) for a bare target; $R_{\mathrm{th}}^{\mathrm{cd}}$, $R_{\mathrm{fast}}^{\mathrm{cd}}$ and $R_{\mathrm{tot}}^{\mathrm{cd}}$ are the reac-

Table 8. Nuclear data used for determination of α-shape parameter

Monitor	$\overline{E}_r$ (eV)[30]	Q_0 [30]	$G=G_{\mathrm{epi}}/G_{\mathrm{th}}$ [19]	F_{cd} [31]	g [32]
^{197}Au	5.65	15.7	0.24 ±0.01	1.009	1.0054
^{63}Cu	1040	1.14	0.72 ±0.02	1.000	1.0002

Table 9. The values of the α-shape parameter obtained from different equations

α shape parameter		
[29]	[25, 26]	Present work
–0.0589 ±0.012	–0.0784 ±0.012	–0.0841 ±0.012

Table 10. The experimental value of α shape parameter for the different monitor pair

Monitor pair	α^{exp} (before correction)	a^{corr} (after correction)
^{197}Au - ^{63}Cu	–0.084 ±0.009	–0.055 ±0.010
α-shape parameter deduced from MCNP simulatedneutron spectrum	–0.058	

tion rates induced by thermal, fast and all neutrons respectively, for a cadmium covered target.

By using MCNP code, the values of R_{fast}^{bare}, R_{tot}^{bare}, R_{th}^{cd}, R_{fast}^{cd} and R_{tot}^{cd} can be obtained and therefore, it is possible to determine the correction factors coefficients C_f^{bare} and C_{tf}^{cd}. The reaction rates and cadmium ratios obtained from the experiment will be corrected by using the following formulas

$$R_{corr}^{bare} = R^{bare}(1-C_f^{bare}) \quad (14)$$

$$R_{corr}^{cd} = R^{cd}(1-C_{tf}^{cd}) \quad (15)$$

$$CR_{corr}^{exp} = \frac{(1-C_f^{bare})}{(1-C_{tf}^{cd})} CR^{exp} \quad (16)$$

By applying our suggested correction factors, the values of the α-shape parameter were recalculated using eq. (11), where CR was replaced by CR_{corr}^{exp}, calculated by eq. (16). The obtained corrected α shape parameter is listed in tab.10 for comparison. It can be seen immediately that the difference between the experimental and calculated values of α-shape parameter, after applying the correction proposed by us, was reduced quite a lot. This indicates that our proposed corrections are meaningful.

CONCLUSIONS

In this article, the results of the determination of the characteristics of the neutron spectrum, at different irradiation locations, using simulation methods, have been presented. The characteristics of neutron spectrum at the irradiation positions including the flux of thermal, epithermal and fast neutron, neutron temperature and α-shape parameter can be determined from the neutron spectra simulated by MCNP code. The results obtained from the simulation were compared with the corresponding results deduced from the experiment to confirm the accuracy of the MCNP code. The comparison shows that the results obtained from MCNP simulation are quite consistent with experimental measurements using the activation method except for α-shape parameter. The values of α-shape parameter at an irradiation position measured by different monitor pairs are very different when comparing each other and different from the value deduced from MCNP simulation. A correction method has been for the experimental determination of α-shape parameter. After applying this correction, the difference of the values of coefficient α-shape parameter measured experimentally is significantly reduced, proving the effectiveness of the proposed correction method.

ACKNOWLEDGMENT

The authors acknowledge partial financial support from the Vietnam Ministry of Science and Technology through Grant DTCB.06/25/ TTDTHN and the Vietnam Academy of Science and Technology for support for senior researchers (Grant No. NVCC05.01/24-25). The support from the Plenipotentiary of Vietnam to JINR for our collaboration is highly appreciated. The authors are indebted to the IREN staffs for their careful operation of the accelerator.

AUTHOR'S CONTRIBUTIONS

L. H. Khiem, supervised, analyzed the data and wrote the manuscript; L. T. M. Nhat, V. D. Cong, P. T. Thanh, T. N. Toan, T. H. B. Phi, V. V. Lobachev: simulation and performed measurements; N. T. Dinh, N. T. X. Thai, N. A. Son, D. V. Trung. N. T. Binh: analyzed the data; V. N. Shvetsov, A. Yu. Dmitriev and S. B. Borzakov reviewed and edited the manuscript.

ORCID NO

L. T. M. Nhat: 0000-0003-2964-0506
V. D. Cong: 0000-0002-0174-4728
L. H. Khiem: 0000-0001-6869-8976
N. T. Dinh: 0009-0009-6275-5752
P. T. Thanh: 0009-0000-1709-9244
T. H. B. Phi: 0009-0009-3200-8502
N. T. X. Thai: 0009-0007-4517-4361
T. N. Toan: 0000-0002-7641-8679
D. V. Trung: 0000-0003-3650-4908
N. T. Binh: 0000-0001-9055-8291
N. A. Son: 0000-0003-2108-439X
V. N. Shvetsov: 0000-0001-8958-0117
A. Yu. Dmitriev: 0000-0002-6163-5128
V. V. Lobachev: 0009-0009-1757-4418
S. B. Borzakov: 0000-0002-2169-0114

REFERENCE

[1] Reifarth, R., *et al*., Neutron-induced Cross Sections, *Eur Phys J Plus, 133* (2018), 424
[2] Belikov, O. V., *et al*., Physical Start-up of the First Stage of IREN Facility, *J Phys: Conf Ser, 205* (2010), 012053
[3] Boettcher, Ju., *et al*., LUE-200 Accelerator of IREN Facility: Current Status and Development, *Phys Part Nucl Lett, 11* (2014), 5, pp. 665-671

[4] Shvetsov, V. N., Neutron Sources at the Frank Laboratory of Neutron Physics of the Joint Institute for Nuclear Research, *Quantum Beam Sci, 1* (2017), 1, 6
[5] Khattab, K., *et al*., Calculations of the Thermal and Fast Neutron Fluxes in the Syrian Miniature Neutron Source Reactor Using the MCNP-4C Code, *Appl Radiat Isot, 67* (2009), 4, pp. 535-538
[6] Akaho, E. H. K., *et al.*, Characterization of Neutron Flux Spectra in Irradiation Sites of MNSR Reactor Using the Westcott-formalism for the k0 Neutron Activation Analysis Method, *Appl Radiat Isot, 57* (2002), 2, pp. 265-273
[7] Beasley, D. G., *et al*., Characterisation of the Epithermal Neutron Irradiation Facility at the Portuguese Reactor Using MCNP, *Appl Radiat Isot, 99* (2015), May, pp. 186-192
[8] Dias, M. S., *et al*., Determination of the Neutron Spectrum Shape Parameter α in k_0 NAA Methodology Using Covariance Analysis, *Appl Radiat Isot, 68* (2010), 4.5, pp. 592-595
[9] Yavar, A. R., *et al*., Verification of MCNP Simulation of Neutron Flux Parameters at TRIGA MK II Reactor of Malaysia, *Appl Radiat Isot, 70* (2012), 10, pp. 2488-2493
[10] Soleimani, B., *et al*., Determination of Neutron Flux Parameters (f, α, φth and φe) of the Irradiation Sites of Isfahan MNSR Reactor Using Empirical and MCNPX2.6 Simulation Approaches, *Appl Radiat Isot, 148* (2019), June, pp. 80-86
[11] Alloni, D., e*t al*., Characterisation of the Secondary Neutron Field Generated by a Compact PET Cyclotron with MCNP6 and Experimental Measurements, *Appl Radiat Isot, 128* (2017), Oct., pp. 204-209
[12] Devan, K., et. al., Photo-Neutrons Produced at the Pohang Neutron Facility Based on an Electron Linac, *J Korean Phys Soc, 49* (2006), 1, pp. 89-96
[13] Sari, A., Characterization of Photoneutron Fluxes Emitted by Electron Accelerators in the 4. 20 MeV Range Using Monte Carlo Codes: A Critical Review, *Appl Radiat Isot, 191* (2023), 110506
[14] Pelowitz, D. B. (Ed.), MCNP6 User fs Manual, Version 1.0, Los Alamos National Laboratory, Report LA-CP-11-01708, 2012
[15] Sumbaev, A., *et al*., LUE-200 Accelerator – A Photo-neutron Generator for the Pulsed Neutron Source "IREN", *J Instrum, 15* (2020), T11006
[16] Nguyen, V. D., *et al*., Measurements of Neutron and Photon Distributions by Using an Activation Technique at the Pohang Neutron Facility, *J Korean Phys Soc, 48* (2006), 3, pp. 382-389
[17] Sudar, S., "TRUECOINC", A Software Utility for Calculation of the True Coincidence Correction, IAEA-Techdoc, 1275, 2002, pp. 37- 48
[18] Trkov, A., *et al*., Nuclear Reactions and Physical Models for Neutron Activation Analysis, *J Radioanal Nucl Chem, 304* (2015), 2, pp. 763-778
[19] Trkov, A., *et al*., On the Self-shielding Factors in Neutron Activation Analysis, *Nucl Instrum Methods Phys Res Sect A, 610* (2009), 2, pp. 553-565
[20] ***IAEA, Neutron Fluence Measurements, Technical Reports Series No. 107, IAEA, Vienna, 1970
[21] De Corte, F., *et al*., Modification and Generalization of some Methods to Improve the Accuracy of α-determination in the $1/E^{1+\alpha}$ Epithermal Neutron Spectrum, *J Radioanal Nucl Chem, 52* (1979), 2, pp. 305-317
[22] Zangirolami, D. M., *et al*., Thermal and Epithermal Neutron Fluence Rates in the Irradiation Facilities of the TRIGA IPR-R1 Nuclear Reactor, *Braz J Phys, 40* (2010), 1, pp. 47-51
[23] Kuo, W. S., Evaluation of Cadmium Ratio for Conceptual Design of a Cyclotron Based Thermal Neutron Radiography System, *Nucl Eng Technol, 54* (2022), 7, pp. 2572-2578
[24] Ryves, T. B., A New Thermal Neutron Flux Convention, *Metrologia, 5* (1969), 4, pp. 119-124
[25] Yucel, M. H, *et al*., Experimental Determination of the α-shape Factor in the $1/E^{1+\alpha}$ Epithermalisotopic Neutron Source-spectrum by Dual Monitor Method, *Ann Nucl Energy, 31* (2004), 6, pp. 681-695
[26] Nguyen, V. D., *et al.*, Measurement of Thermal Neutron Cross-section and Resonance Integral for the ^{165}Ho(n, γ)^{166g}Ho Reaction Using Electron Linac-based Neutron Source, *Nucl Instrum Methods Phys Res Sect B, 269* (2011), 2, pp. 159.166
[27] Blaauw, M., *et al*., The Confusing Issue of the Neutron Capture Cross-section to Use in Thermal Neutron Self-shielding Computations, *Nucl Instrum Methods Phys Res A, 356* (1995), 2-3, pp. 403-407
[28] Martinho, E., *et al*., Universal Curve of Epithermal Neutron Self-shielding Factor in Foils, Wires and Spheres, *Appl Radiatand Isot, 58* (2003), 3, pp. 371-375
[29] Karadag, M., *et al*., Measurement of Thermal Neutron Cross-sections and Resonance Integrals for ^{71}Ga(n, γ)^{72}Ga and ^{75}As(n, γ)^{76}As by Using ^{241}Am-Be Isotopic Neutron Source, *Nucl Instrum Methods Phys Res Sect A, 501* (2003), 2-3, pp. 524-535
[30] De Corte, F., *et al*., Recommended Nuclear Data for Use in the ko Standardization of Neutron Activation Analysis, *At Data Nucl Data Tables, 85* (2003), 1, pp. 47-67
[31] El Nimr, T., *et al*., Epicadmium Neutron Activation Analysis (ENAA) Based on the k_0-Comparator Method, *J Radioanal Nucl Chem, 67* (1981), 2, pp. 421-435
[32] Mughabghab, S. F., Thermal Neutron Capture Cross Sections Resonance Integrals and g-Factors, Report Number INDC(NDS)-440, IAEA, Vienna, 2003

Received on March 29, 2025
Accepted on may 19, 2025

Ле Тран Мињ ЊАТ, Ву Дук КОНГ, Ле Хонг КИМ, Нгујен Ти ДИЊ, Фам Тин ТАЊ, Труенг Хоаи Бао ФИ, Нгујен Ти Шуен ТАИ, Тран Нгок ТОАН, Дињ Ван ТРУНГ, Нгујен Тањ БИЊ, Нгујен Ан СОН, Валери Николајевич ШЕЦОВ, Андреј Јуриевич ДМИТРИЈЕВ, Валериј Владимирович ЛОБАЧЕВ, Сергеј Борисович БОРЗАКОВ

ОДРЕЂИВАЊЕ ПАРАМЕТАРА НЕУТРОНСКОГ СПЕКТРА У ПОСТРОЈЕЊУ IREN КОРИШЋЕЊЕМ MCNP СИМУЛАЦИЈЕ И ЕКСПЕРИМЕНТАЛНЕ ПОТВРДЕ

Приказано је одређивање карактеристика неутронског спектра са различитим позицијама зрачења на спољашњем зиду модераторске коморе интензивног резонантног неутронског извора, методом симулације MCNP кодом. Одређене су карактеристике неутронског спектра, укључујући флукс термичких, епитермичких и брзих неутрона, температуру неутрона и параметар α-облика. За потврду MCNP симулације, карактеристике неутронског спектра на оптималној позицији зрачења одређене су експериментално техником активације. Поређење показује да се симулирани и експериментални резултати слажу, што указује на високу поузданост MCNP кода, осим за параметар α-облика. Ради побољшања тачности, коришћена је овде ревидирана једначина за одређивање параметра α-облика методом кадмијум односа за више монитора, у коју су укључени коефицијенти корекције преноса епитермичких неутрона за кадмијумски премаз, термичку и епитермичку самозаштиту неутрона. Израчунати и измерени параметри α-облика у доброј су сагласности када се користи овде предложена ревидирана једначина.

Кључне речи: интензивни резонантни неутронски извор, карактеризација неутронског спектра, MCNP програм, метода активације